Pergamon

Geochimica et Cosmochimica Acta, Vol. 68, No. 20, pp. 4099-4111, 2004

0016-7037/04 $30.00 + .00

doi:10.1016/j.gca.2004.04.005

Factors affecting dissolved organic matter dynamics in mixed-redox to anoxic coastal sediments

TOMOKO KOMADA,[1,†,*] CLARE E. REIMERS,[2] GEORGE W. LUTHER III[3] and DAVID J. BURDIGE[4]

[1]Institute of Marine and Coastal Sciences, Rutgers The State University of New Jersey, New Brunswick, NJ 08904, USA
[2]College of Oceanic and Atmospheric Sciences, Oregon State University, Corvallis, OR 97331, USA
[3]College of Marine Studies, University of Delaware, Lewes, DE 19958, USA
[4]Department of Ocean, Earth and Atmospheric Sciences, Old Dominion University, Norfolk, VA 23529, USA

(*Received October* 13, 2003; *accepted in revised form April* 7, 2004)

Abstract—Mixed-redox (suboxic, or oscillating between oxidizing and reducing conditions) to anoxic marine sediments from the Raritan –New York Bay complex and the Inner New York Bight of the eastern U.S. were studied to investigate the factors controlling the accumulation of pore-water dissolved organic carbon (DOC). DOC increased with depth at each of four study sites, but accumulation was generally limited in the mixed-redox zone relative to the anoxic zone. Humic-like fluorescence intensity also differed between mixed-redox and anoxic zones of the sediment, such that anoxic pore waters were relatively enriched in fluorescent, humic-like compounds.

A pore-water DOC model was tested for its capacity to explain these geochemical patterns. Model results for a heavily irrigated and a non-bioturbated site both suggest that, excluding the uppermost few cm of the sediment column, pore-water DOC is predominantly comprised of poorly-reactive material with estimated degradation rate constants on the order of 10^{-3} yr^{-1}. Model results are also consistent with the suggestion that DOC accumulation is suppressed in the mixed-redox compared to the anoxic zones of the sediment due to rapid oxidation of high-molecular-weight DOC, and limited production and enhanced oxidation of the less reactive polymeric low-molecular-weight component of the DOC pool. An assessment of sorptive behavior of DOC in the surface sediments of the study area suggests that sorption can influence pore-water DOC distributions under conditions of high sedimentation and low bioirrigation. *Copyright © 2004 Elsevier Ltd*

1. INTRODUCTION

Dissolved organic carbon (DOC) is produced in marine sediments as an intermediate in the mineralization of organic matter (Henrichs, 1992; Alperin et al., 1994). Fluxes of DOC across the sediment-water interface suggest that net DOC production within marine sediments constitutes an important component of the marine organic carbon (OC) budget (Burdige et al., 1999; Holcombe et al., 2001). Identification of key reaction and transport processes that affect pore-water DOC distributions is therefore critical in assessing the controls on OC mineralization in sediments, and the significance of benthic metabolism in the oceanic OC cycle. However, such a task can be difficult because DOC is a complex mixture of various components exhibiting a range in reactivities (e.g., Henrichs and Farrington, 1979; Sansone and Martens, 1982; Chin and Gschwend, 1991; Arnosti and Holmer, 1999; Hee et al., 2001).

Despite this complexity, Alperin et al. (1994) successfully modeled seasonal dynamics in an organic-rich anoxic sediment by identifying two subpools of DOC: acid-volatile and non-acid-volatile components. More recently, Burdige (2002) demonstrated that a first order understanding of the factors that influence DOC distribution and cycling in mixed-redox (suboxic, or oscillating between oxidizing and reducing conditions) to anoxic sediments may be gained by modeling DOC as a mixture of a labile, high-molecular-weight component (HMW-DOC), and a less reactive, polymeric low-molecular-weight component (pLMW-DOC). In this model, HMW-DOC is initially produced from sediment particulate OC (POC) by microbial hydrolysis or oxidative cleavage. A large fraction (~90%) of HMW-DOC is then rapidly oxidized to dissolved inorganic carbon (DIC) via monomeric, low-molecular-weight DOC. Meanwhile, the remaining fraction of HMW-DOC is converted to pLMW-DOC which subsequently accumulates in the pore water due to its low reactivity.

One important prediction of the Burdige (2002) model is that the majority of the DOC accumulating in sediment pore waters consists of relatively non-reactive pLMW-DOC, while the more labile HMW-DOC is quantitatively significant only near the sediment surface where the mineralization rate of POC is usually at a maximum. Based on biogeochemical data from two locations in the Chesapeake Bay, Burdige (2001) further observed that the accumulation of DOC was suppressed in mixed-redox sediments relative to persistently anoxic sediments. This suppression may result from enhanced oxidation and/or lowered production of pLMW-DOC, analogous to enhanced POC degradation under mixed-redox conditions (Aller, 1994). Model results presented by Burdige (2002) are consistent with these observations but require additional validation with field data.

The objective of this study was to test and further advance the DOC cycling model formulated by Burdige (2002) using biogeochemical data from the Hudson River Estuary and the Inner New York Bight sediments. For this purpose, the model was modified to explicitly incorporate DIC and NH_4^+ in addi-

* Author to whom correspondence should be addressed (tkomada@sfsu.edu).
† *Present address:* Romberg Tiburon Center for Environmental Studies, San Francisco State University, 3152 Paradise Drive, Tiburon, CA 94920.

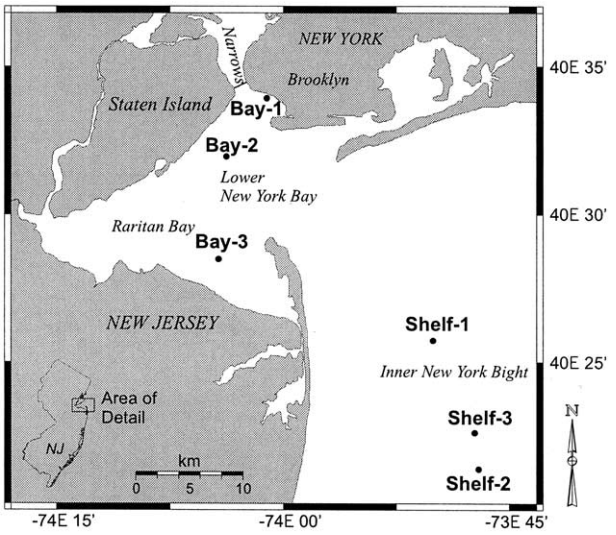

Fig. 1. Sampling locations in the Raritan–Lower New York Bay complex and the Inner New York Bight. Sediment cores were collected for this study from the three Bay stations and Shelf-3. Partitioning behavior of OC was examined in a related study using surface sediments collected from stations Bay-1 to Bay-3 and Shelf-1 and Shelf-2.

tion to the two DOC pools, HMW- and pLMW-DOC. Specific objectives were:

1. Determine whether the bulk of the pore-water DOC is of low reactivity, and whether the cycling of this material differs under different redox conditions.
2. Adsorption and desorption were not considered in the original model, but the potential of these processes to influence DOC dynamics has been stated previously (Hedges and Keil, 1995; Thimsen and Keil, 1998). Thus, the second objective was to extend the model to evaluate the role of adsorption and desorption in pore-water DOC cycling.

2. DATA SET

2.1. Station Locations, Sampling, and Analyses

Sediment cores and bottom water samples were collected from four stations in the Raritan–New York Bay complex (stations Bay-1 to Bay-3) and the Inner New York Bight (station Shelf-3; Fig. 1; Table 1). A macrobenthic invertebrate survey conducted in the vicinity of Bay-3 showed dominance of the crustacean *Ampelisca vadorum* along with various tube-building oligochaete and polychaete worms (J. Gregg, unpublished data). X-radiograph images obtained for stations Bay-3 and Shelf-3 indicated the presence of deep (>25 cm) burrow structures at station Bay-3, while irrigation and bioturbation appeared negligible at station Shelf-3. The overall lack of bioturbation and deep irrigation at Shelf-3 have been confirmed further with macrofaunal abundance and ^{210}Pb and ^{137}Cs profiles (M. ten Brink, private communication). However, a negative anomaly in ^{210}Pb activity within the uppermost few centimeters of the sediment indicated that a pulse of fine-grained sediment was deposited at Shelf-3 in the recent past (M. ten Brink, private communication). This is likely due to energetic currents that have been documented to re-distribute surface sediments in this region of the upper Hudson Shelf Valley (Harris et al., 2003). Bottom- and pore-water samples (DIC, nutrients, DOC, total Fe and Mn, total sulfide, and humic-like fluorescence) and solid sediment (Fe oxyhydroxides, acid volatile sulfide) were analyzed using procedures adapted from the literature and are summarized in Appendix A.

2.2. Pore Water and Solid Phase Profiles

2.2.1. DIC and NH_4^+ Accumulation and Redox Regime

High rates of organic matter remineralization were indicated by the curvature of DIC and nutrient profiles at all stations (Figs. 2 and 3). DIC and NH_4^+ profiles tended to co-vary, and generally increased steadily with depth (Figs. 2 and 3). Consistent with the X-radiograph images discussed above, Bay-3 appeared to be strongly impacted by bioirrigation based on distinct subsurface minima in the NH_4^+ and DIC profiles (Fig. 3).

Oxygen penetration depths at the Bay stations were measured in situ by microelectrodes, and were generally 2 to 4 mm (Luther et al., 1999). High levels of pore-water Mn and Fe in the uppermost 5–10 cm of the Bay sediments indicated the occurrence of mixed-redox diagenesis (Fig. 2). Sulfate reduction was also significant based on the accumulation of NH_4^+

Table 1. Summary of bottom-water[a] and sediment-core sampling.

Station	Lat (N), Lon (W)	Depth (m)	Date of sampling	Salinity[b]	Bottom T[b] (°C)	Coring method[c]	PW sampling method[d]
Bay-1	40.596,74.002	5	6/26/98	24	21	Grab	Slice
Bay-2	40.549,74.064	8	6/28/98	27	19	Push core	Slice
Bay-3	40.458,74.074	6	6/27/97	27	20	HGC	Squeeze
			6/25/98	23	20	Grab	Slice
			7/22/99	28	n.a.	Gravity	Slice
			8/3/99	28	n.a.	Grab	Slice
Shelf-3	40.317,73.791	50	6/26/97	32	9	HGC	Squeeze

n.a. = not available.
[a] Collected using a Niskin bottle.
[b] Determined with a CTD.
[c] Grab = Peterson grab sampler; Push core = a push core mounted on a remotely operated vehicle; HGC = hydrostatically-damped gravity corer built by the U.S. Geological Survey; Gravity = gravity corer.
[d] Sliced cores were processed in a N_2 atmosphere and centrifuged as described in Komada and Reimers (2001). DOC concentrations of pore waters recovered using this method agreed well with those obtained by sipping (Komada, unpublished data), suggesting that DOC contamination by cell rupture (Alperin et al., 1999) was minimal. Squeezed cores were processed on deck using a squeezer similar to that reported by Jahnke (1988).

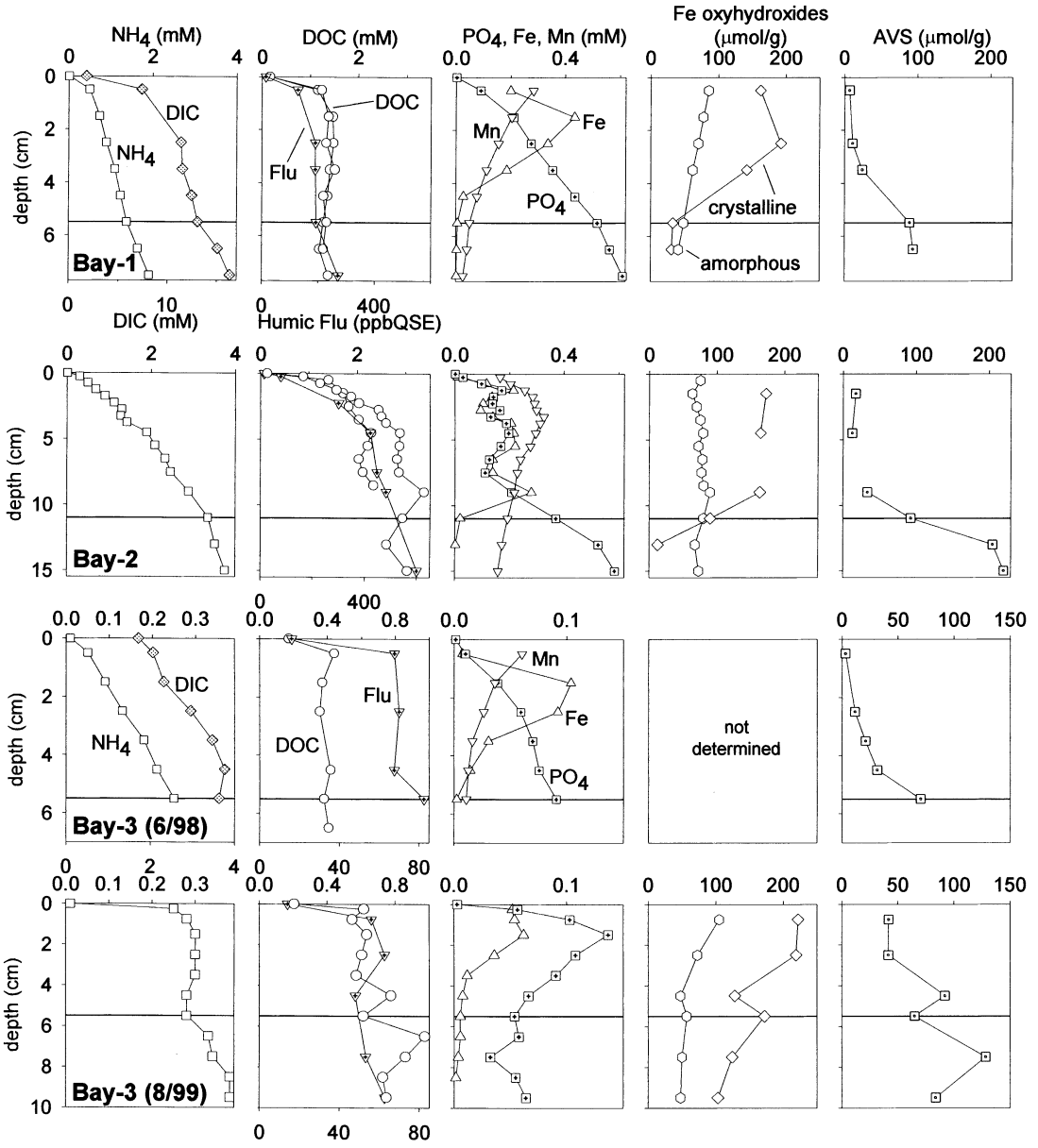

Fig. 2. Short (<15 cm) profiles from stations Bay-1, Bay-2 and Bay-3. Humic Flu = humic-like fluorescence, AVS = acid volatile sulfide, horizontal lines = estimated mixed-redox/anoxic boundary. Replicate DOC profiles from two cores are presented for stations Bay-1 and Bay-2.

and acid volatile sulfide (AVS; Figs. 2 and 3). Dissolved sulfide was present at levels as high as 1.5 mmol/L at Shelf-3 (Fig. 3), but was not detectable to a depth of 30 cm at station Bay-3 in 7/99. The mirror image distributions of AVS and Fe oxyhydroxides (Fig. 2) suggest that oxidized iron reacted rapidly with dissolved sulfide to form AVS.

To fulfill our goal of assessing pore-water DOC dynamics across a redox gradient, a reference horizon that separates mixed-redox and permanently anoxic sediments is needed. Assuming that the primary sink for dissolved Fe is precipitation as sulfides, we will use the depth where dissolved Fe disappears as an approximation for the boundary between mixed-redox and anoxic sediments. For station Shelf-3 where dissolved Fe data are not available, the depth where free sulfide begins to accumulate will be used to estimate this redox boundary.

2.2.2. *Accumulation Patterns of DOC*

Over a depth scale on the order of 10 cm, DOC concentration increased steadily with DIC and NH_4^+ (Fig. 3), similar to trends reported previously for anoxic coastal sediments (e.g., Alperin et al., 1994; Burdige and Homstead, 1994). In contrast, DOC appeared to remain constant (at a concentration greater than that of the overlying water) from the sediment-water interface to several centimeters beyond the mixed-redox/anoxic boundary (Figs. 2 and 3). This apparent lack of early DOC

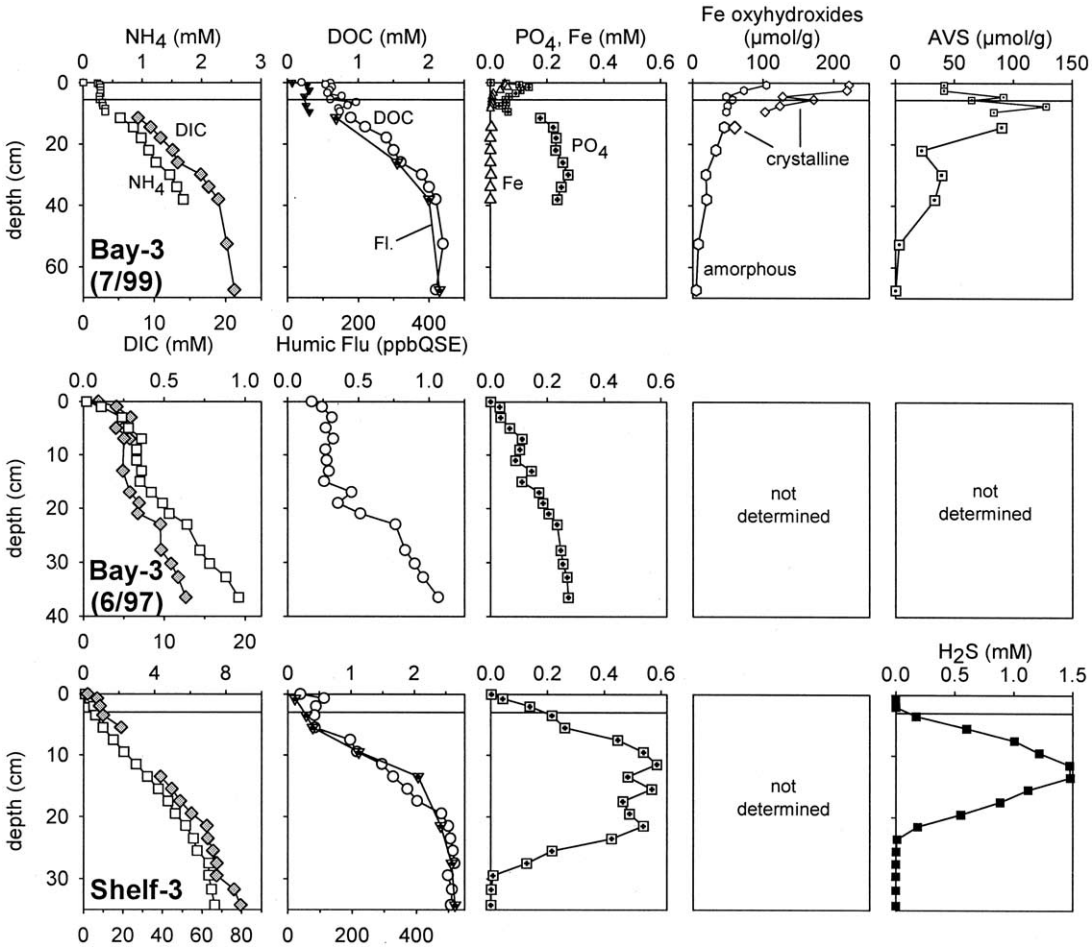

Fig. 3. Long (>15 cm) profiles from stations Bay-3 (7/99 and 6/97) and Shelf-3. Note that total dissolved sulfide is shown instead of AVS in the right-most column for station Shelf-3. Small symbols in the Bay-3 (7/99) profiles are reproductions of Bay-3 (8/99) given in Figure 2. The horizontal lines indicate the estimated mixed-redox/anoxic boundary.

accumulation with depth was observed at all stations except the heavily bioirrigated Bay-3 (8/99 and 6/97), and Bay-2 where DOC increased steadily to ~5 cm depth (Figs. 2 and 3). These patterns have been observed in other mixed-redox marine sediments (e.g., Sholkovitz and Mann, 1984; Martin and McCorkle, 1993; Bauer et al., 1995), and appear consistent with the hypothesis that mixed-redox conditions enhance consumption and/or lowers production of DOC relative to anoxic conditions (Burdige, 2001).

2.2.3. *Fluorescence Profiles*

When excited with UV light, humic-like organic matter in aquatic environments commonly exhibits broad, featureless fluorescence in the blue region of the spectrum (e.g., Laane and Koole, 1982; Chen and Bada, 1989; Coble, 1996). Based on the tendency for humic-like fluorescence to closely parallel pore-water DOC (Chen et al., 1993; Chen and Bada, 1994), it has been suggested that pLMW-DOC and humic-like substances may be synonymous (Burdige, 2002; Burdige et al., 2004).

To investigate the depth distribution of the humic-like components of pore-water DOC, fluorescence properties of pore-water dissolved organic matter were examined by excitation-emission matrix fluorescence spectroscopy (Coble, 1996; Appendix A). Humic-like peaks (defined as maximum emission [*Em*] at maximum excitation [*Ex*]) were observed at all stations and depths, and were all positioned near *Ex*/*Em* 310/420 nm (Komada et al., 2002), close to previously reported humic-like peak positions (Coble, 1996). Peak intensity increased with depth, and in general, co-varied with bulk DOC (Figs. 2 and 3) similar to what has been reported for other marine sediments (Chen et al., 1993; Chen and Bada, 1994; Burdige et al., 2004).

However, closer inspection of the data revealed that fluorescence properties of pore-water DOC differ above and below the mixed-redox/anoxic boundaries. First, in agreement with a previous report (Chen and Bada, 1994), anoxic pore waters were enriched in fluorescent humic-like substances relative to mixed-redox pore waters ($p = 0.05$; Fig. 4). Second, the ratio r = (maximum *Em* at *Ex* 360 nm)/(maximum *Em* at *Ex* 310 nm) increased significantly ($p = 0.05$) from 0.66 ± 0.07 in the mixed-redox to 0.76 ± 0.04 in the anoxic zone. r has been used previously as an indicator for degraded and/or aged organic matter in the DOC pool (Komada et al., 2002)

If humic-like fluorescence is indeed representative of

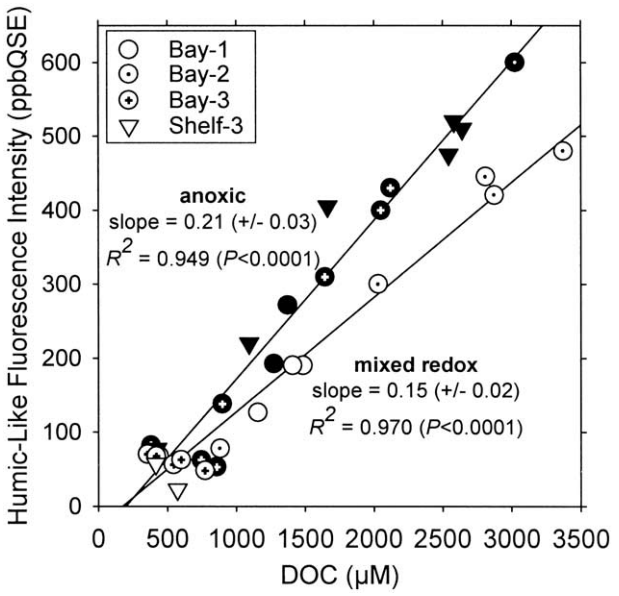

Fig. 4. Maximum intensity of humic-like fluorescence versus DOC concentration. White and black symbols are those collected from above and below the mixed-redox/anoxic boundary (horizontal lines in Figs. 2 and 3; see section 2.2 for definition), respectively.

pLMW-DOC, then these results are consistent with a model in which pLMW-DOC is a quantitatively significant fraction of pore-water DOC, and that its accumulation is suppressed under mixed-redox relative to anoxic conditions in the sediment column.

2.3. Partitioning of OC Between Pore Water and Sediment Particles

In a related study using sediments from the same region (Fig. 1), it was determined that ~0.1% of the surface sediment POC (0–2 cm) is readily released into solution when suspended in bottom water for 1 h (Table 2; Komada and Reimers, 2001). A positive correlation between the amount of OC released and POC of the high-density phase ($\rho > 1.9$) of the sediment further suggested that OC in association with the mineral particles was the major source for the released OC (Komada and Reimers, 2001).

We used the data reported by Komada and Reimers (2001) to derive a dimensionless partition coefficient (K) for DOC. K was calculated using a linear adsorption model (Berner, 1980):

$$K = \rho_s \left(\frac{1-\phi}{\phi} \right) K_{ads} \quad (1)$$

where ρ_s is the density of sediment solids (assumed to be 2.5 g cm^{-3}), ϕ is the porosity, and K_{ads} is the partition coefficient with dimensions of L g^{-1} (Table 2). K_{ads} was determined for the surface sediments by dividing the readily-releasable fraction of POC (μmol OC g dry $sediment^{-1}$) by the DOC concentration of the pore solution (μmol/L) (Table 2). Eqn. 1 assumes that the sorptive behavior of DOC can be represented with a unique K, which is likely to be an oversimplification (Thimsen and Keil, 1998; Arnarson and Keil, 2000). Also, because the experiments of Komada and Reimers (2001) were conducted under oxic conditions, the results reported in Table 2 may not be fully applicable to anoxic sediments; previous sorption studies have generally shown lower values of K under anoxic compared to oxic conditions (Wang and Lee, 1993; Montluçon and Lee, 2001). Despite these limitations, we use the linear model (Eqn. 1) as a first order approach to estimate the influence of adsorption on pore-water DOC distributions.

The resulting values of K were similar across stations and ranged from 0.8 to 1.3 (Table 2). To compare these results to previously published values, the adsorption coefficients reported by Thimsen and Keil (1998) and Arnarson and Keil (2000) (determined under oxic conditions) were converted to non-dimensional form by applying their experimental slurry porosities and an assumed sediment solid density of 2.5 g cm^{-3} to Eqn. 1. The resulting values of K for Thimsen and Keil (1998) and Arnarson and Keil (2000) are 0.04 to 6.4 and 0.4 to 0.9, respectively. These values overlap with our estimates, and are similar to non-dimensional partition coefficients reported for melanoidin in oxic coastal sediments (~2; Montluçon and Lee, 2001). Together, these observations indicate that $K = 1$ should be an appropriate estimate for the pore-water DOC model.

Table 2. Estimated equilibrium partition coefficients of DOC in surficial (uppermost 2 cm) sediments.

	Experimental data[a]			Core sectioning data (uppermost 2 cm)			
Station	HD-POC[b] (wt.%)	Mass-normalized OC release (μmol g^{-1})	Fraction of HD-POC released (%)	Av. pore water DOC μmol/L	Av. porosity	K_{ads}[c] (10^{-3} L g^{-1})	K[d]
Bay-1	3.76	2.58	0.08	1310	0.84	2.0	0.9
Bay-2	4.26	3.73	0.11	1443	0.84	2.6	1.2
Bay-3	2.89	0.71	0.03	405	0.77	1.8	1.3
Shelf-1	1.88	1.14	0.07	1164	0.69	1.0	1.1
Shelf-2	3.71	3.84	0.12	1678	0.88	2.3	0.8

[a] Data from Komada and Reimers (2001).
[b] POC content in the high-density ($\rho > 1.9$) phase of the sediment matrix.
[c] Partition coefficient determined by dividing column 3 by column 5 (section 2.3).
[d] Non-dimensional partition coefficient derived using Eqn. 1.

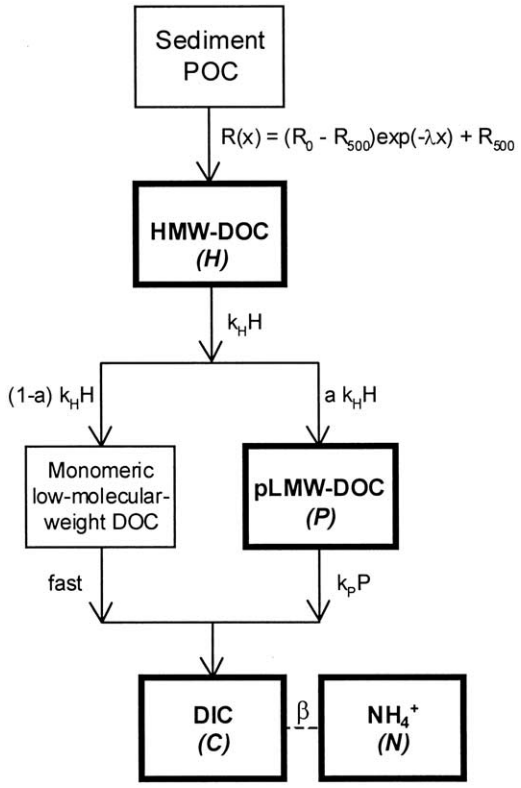

Fig. 5. A schematic of the coupled DOC-DIC-NH_4^+ model modified after the pore-water DOC model developed by Burdige (2002). Symbols are explained in Table 3. *N* is calculated from *C* by applying a molar production ratio, β. Explicitly modeled components are indicated in bold.

3. Development of a Coupled DOC-DIC-NH_4^+ Model

In the steady state, advection/reaction/diffusion model for pore-water DOC (Burdige, 2002), a reactive high-molecular-weight intermediate, HMW-DOC, is first produced from POC. The production rate of HMW-DOC decreases exponentially with depth to a constant value. Most of the HMW-DOC is then rapidly oxidized to DIC via its reactive monomeric components, but a small fraction is shunted into a less reactive, polymeric pool which subsequently accumulates in the pore water. To explain the observation that DOC concentrations generally approach asymptotic values with depth in the sediment (e.g., Burdige and Homstead, 1994; Alperin et al., 1994, 1999), the production rate of pLMW-DOC at depth is balanced by its rate of oxidation to DIC.

In the present study, two main modifications were made to the Burdige (2002) DOC model. First, to better constrain the unknown parameters, DIC and NH_4^+ concentrations were modeled simultaneously with HMW- and pLMW-DOC (Fig. 5). Second, the effect of linear adsorption of DOC was incorporated. Adopting these modifications, one-dimensional diagenetic equations assuming steady state, no compaction, and constant porosity can be written for HMW-DOC (*H*), pLMW-DOC (*P*), DIC (*C*), and NH_4^+ (*N*) as (Berner, 1980; Boudreau, 1997):

$$\frac{d}{dx}\left[\left[(1+K)D_B + D_H^e\right]\frac{dH}{dx}\right] - (1+K)\omega\frac{dH}{dx} + \alpha(H_0 - H) + R(x) - k_H H = 0 \quad (2)$$

$$\frac{d}{dx}\left[\left[(1+K)D_B + D_P^e\right]\frac{dP}{dx}\right] - (1+K)\omega\frac{dP}{dx} + \alpha(P_0 - P) + ak_H H - k_p P = 0 \quad (3)$$

$$D_C^e\frac{d^2C}{dx^2} - \omega\frac{dC}{dx} + \alpha\left(C_0 - C\right) + \left(1-a\right)k_H H + k_p P = 0 \quad (4)$$

$$D_N^e\frac{d^2N}{dx^2} - \left(1+K_N\right)\omega\frac{dN}{dx} + \alpha\left(N_0 - N\right) + \beta\left[\left(1-a\right)k_H H + k_p P\right] = 0 \quad (5)$$

where *x* is the depth below the sediment-water interface, D_B is the biodiffusion coefficient for interphase mixing, D^e_i (i = *H*, *P*, *C*, *N*) is the effective molecular diffusion coefficient corrected for tortuosity, *K* is the dimensionless linear adsorption constant for HMW- and pLMW-DOC, ω is the sedimentation rate, α is the rate constant for bioirrigation represented as a non-local process (Emerson et al., 1984), $R(x)$ is the net production rate for HMW-DOC, *a* is the fraction of HMW-DOC converted to pLMW-DOC, k_H and k_P are rate constants for HMW- and pLMW-DOC degradation, respectively, K_N is the dimensionless linear adsorption constant for NH_4^+, β is the NH_4^+:DIC molar production ratio, and subscript 0 represents values at the sediment-water interface (Tables 3 and 4).

The parameter $R(x)$ is defined to decay exponentially with depth with an attenuation constant λ:

$$R(x) = \left(R_0 - R_{500}\right)\exp\left(-\lambda x\right) + R_{500} \quad (6)$$

where R_0 and R_{500} are values at x = 0 cm and x = 500 cm, respectively. In addition, *a* and k_P are allowed to differ across a depth horizon *L* that marks the mixed-redox/anoxic boundary. Because brief, but periodic shifts in the redox regime can enhance sediment POC decomposition (Aller, 1994), *a* may be reduced above horizon *L* by a factor r_a ($r_a \leq 1$), which assumes that production of pLMW- from HMW-DOC is suppressed under mixed-redox conditions. Similarly, k_P may be enhanced above *L* by a factor r_{kp} ($r_{kp} \geq 1$), implying that pLMW-DOC oxidation is more effective under mixed-redox conditions. Both D_B and α were assumed to be constant above the mixed layer depth (MLD), and zero below. Bioturbation was not included in Eqn. 4 and 5, because D^e_C and D^e_N are expected to be several-fold greater than D_B (Table 4).

Eqn. 2 through 5 were solved numerically using the boundary conditions: $H = H_0$, $P = P_0$, $C = C_0$, $N = N_0$ at x = 0; and assuming that $dH/dx = dP/dx = dC/dx = dN/dx = 0$ at x = 500 cm. The first and second order differentials were discretized using the centered-differencing scheme, and the resulting algebraic equations were solved by gaussian elimination (Boudreau, 1997) using a step size of 0.25 cm to a depth of 500 cm. DOC profiles were computed by summing HMW- and pLMW-DOC. The numerical solutions to Eqn. 2 and 3 have been verified previously (Burdige, 2002). The numerical solutions to Eqn. 4 and 5 were validated against analytical solutions

Table 3. List of symbols used in the model.

Symbol	Unit	Description
a	—	Fraction of H that is converted to P
C	μmol/L	Concentration of DIC.
D_B	cm^2 yr^{-1}	Biodiffusion coefficient; assumed constant within the bioturbated zone
D_i^e	cm^2 yr^{-1}	Effective molecular diffusion coefficient (i = H, P, C, or N; see Table 4)
H	μmol/L	Concentration of high-molecular-weight DOC
K	—	Equilibrium linear partition coefficient for H and P
K_N	—	Equilibrium linear partition coefficient for N
k_H	yr^{-1}	Degradation rate constant for H
k_P	yr^{-1}	Degradation rate constant for P
L	cm	Depth horizon above which $k_{Pr} \geq 1$ and/or $a_r \leq 1$
MLD	cm	Depth horizon above which $D_B > 0$ and/or $\alpha > 0$
N	μmol/L	Concentration of NH_4^+
P	μmol/L	Concentration of polymeric low-molecular-weight DOC
r_a	—	Attenuation factor for a within mixed-redox zone ($r_a \leq 1$)
r_{kp}	—	Enhancement factor for k_P within mixed-redox zone ($r_{kp} \geq 1$)
$R(x)$	μmol/L yr^{-1}	Net H production rate
x	cm	Depth below the sediment-water interface
α	yr^{-1}	Bioirrigation constant within the bioturbated zone
β	—	N to C molar production ratio
λ	cm^{-1}	Depth attenuation constant for $R(x)$
ω	cm yr^{-1}	Sedimentation rate

to their simplified forms where α was set to a constant positive value. The solutions are insensitive to variations in step size.

4. MODEL APPLICATION AND DISCUSSION

Pore-water DOC profiles (Figs. 2 and 3) show that DOC accumulation is typically lower in mixed-redox compared to anoxic portions of the sediment column. Fluorescence data are further consistent with the idea that humic-like moieties comprise a significant fraction of DOC, but are more concentrated below the mixed-redox/anoxic boundary (Fig. 4). Combined, these observations lend support to the hypothesis that the accumulation of the more refractory component of pore-water DOC is suppressed in the mixed-redox relative to persistently anoxic regions of the sediment.

To further test this hypothesis, the coupled DOC-DIC-NH_4^+ model was applied to stations Bay-3 (6/97) and Shelf-3. These stations were selected because of availability of profiles that penetrated both mixed-redox and anoxic sediments.

4.1. Model Application to a Bioturbated/Irrigated Site (Bay-3)

The Bay-3 core collected in 6/97 displayed broad inversions in the DIC, NH_4^+ and DOC profiles between 3 and 16 cm depth (Fig. 3), indicating heavy bioirrigation. We used the apparent depth of bioirrigation (16 cm) as an estimate for the horizon below which sediments were permanently anoxic (horizon L), because depth profiles of redox-sensitive species were not available for this core.

The first step of the model application process was to constrain the sediment POC reaction rate, $R(x)$ and the bioirrigation constant, α. To accomplish this without complication from the unknown parameters governing HMW- and pLMW-DOC, DIC and NH_4^+ were first modeled independently by assuming that neither HMW- nor pLMW-DOC are lost by diffusion and burial before mineralization (Fig. 5). This is equivalent to re-expressing the reaction terms for DIC and NH_4^+ in Eqn. 4 and 5 to $R(x)$ and $\beta \times R(x)$, respectively. R_0, R_{500}, α, and λ were then constrained by directly fitting the model to the DIC and NH_4^+ profiles. To reproduce the inversion in the profiles, it was necessary that any choice of R_0 be counterbalanced by an appropriate α; larger R_0 required larger α. Maximum and minimum estimates of R_0 were set by the size of the interfacial gradient. The higher limit could also be set by the size of α: increasing α enhanced the middepth concentration minimum. Once a pair of R_0 and α was selected, λ and R_{500} were obtained by fine-tuning the overall attenuation.

Using this approach, multiple curves were fit to the DIC and

Table 4. Parameters[a] with prescribed values.

	Values used		
Parameter	Bay-3	Shelf-3	Source
C_0	1856 μmol/L	2100 μmol/L	Measured bottom-water values
N_0	20 μmol/L	89 μmol/L	Measured bottom-water values
H_0	5 μmol/L	5 μmol/L	Burdige (2002)
P_0	165 μmol/L	92 μmol/L	Measured bottom-water DOC less H_0
D_B	30 cm^2 yr^{-1}	0	Bay-3 value was estimated from water depth using an empirical relationship given by Middelburg et al. (1997)
D_H^e, D_P^e	47 cm^2 yr^{-1}	30 cm^{-2} yr^{-1}	Molecular diffusion coefficients are from Alperin et al. (1994) for H and P, and Li and Gregory (1974) for N and C, assuming C is all HCO_3^-. They were then corrected for temperature and salinity according to Li and Gregory (1974) and tortuosity using the modified Weissberg relation (Boudreau, 1997).
D_C^e	250 cm^2 yr^{-1}	161 cm^2 yr^{-1}	
D_N^e	426 cm^2 yr^{-1}	285 cm^2 yr^{-1}	
K_N	1.3	1.3	Mackin and Aller (1984)
ω	0.15 cm yr^{-1}	2 cm yr^{-1}	Olsen et al. (1984), Bopp et al. (1995)

[a] See Table 3 for identification.

Table 5. Parameters[a] used to calculate model outputs for stations Shelf-3 and Bay-3 (6/97).

				Constrained with *C* and *N*					Constrained with DOC and fluorescence							
Case no.	Station	MLD	D_B	α	R_0	R_{500}	λ	β	k_H	k_P	a	r_{kp}	r_a	L	K	k_{POC}[b]
1	Bay-3 (6/97)		30	22	20×10^4	100	0.143	0.12	1000	0.003	0.036	1	1	16	1	0.02
2	Bay-3 (6/97)		30	20	15×10^4	100	0.131	0.12	1000	0.003	0.034	1	1	16	1	0.02
3	Bay-3 (6/97)		30	22	25×10^4	200	0.175	0.12	1000	0.004	0.050	1	1	16	1	0.03
4	Bay-3 (6/97)	16	100			Case-1					Case-1				1	0.02
5	Bay-3 (6/97)		100			Case-2					Case-2				1	0.02
6	Bay-3 (6/97)		100			Case-3					Case-3				1	0.03
7	Bay-3 (6/97)		30			Case-1			1000	0.003	0.036	1	0.3	16	1	0.02
8	Bay-3 (6/97)		30			Case-1			3000	0.003	0.036	1	1	16	1	0.02
9	Shelf-3				5.0×10^4	500	0.058	0.19	1000	0.003	0.020	1	1	3	1	0.12
10	Shelf-3				3.5×10^4	0	0.041	0.19	1000	10^{-4}	0.022	1	1	3	1	0.08
11	Shelf-3				6.0×10^4	500	0.066	0.19	1000	0.003	0.019	1	1	3	1	0.13
12	Shelf-3					Case-9			200	0.003	0.020	1	1	3	1	0.12
13	Shelf-3	0	0	0		Case-9			200	0.003	0.020	1000	1	3	1	0.12
14	Shelf-3					Case-9			200	0.003	0.027	1000	1	7	1	0.12
15	Shelf-3					Case-9			200	0.003	0.028	500	0.1	7	1	0.12
16	Shelf-3					Case-9			200	0.003	0.028	500	0.1	7	0	0.12
17	Shelf-3					Case-9			200	0.003	0.028	500	0.1	7	2	0.12

[a] See Table 3 for definition and Table 4 for additional parameters whose values were prescribed.
[b] Degradation rate constant for sediment POC (yr^{-1}) calculated as the product of ω (Table 4) and λ.

NH_4^+ data with R_0 ranging from 15 to 25×10^4 μmol/L yr^{-1}, and α between 20 and 22 yr^{-1} (Case-1 to Case-3; Table 5, Figs. 6a and 6b). Resulting sediment POC degradation rate constants (k_{POC}; Table 5) were 0.02 to 0.03 yr^{-1}, which overlap with the lower range of values reported for other coastal sediments (Henrichs, 1992). R_0, R_{500}, α, and λ were then applied to the

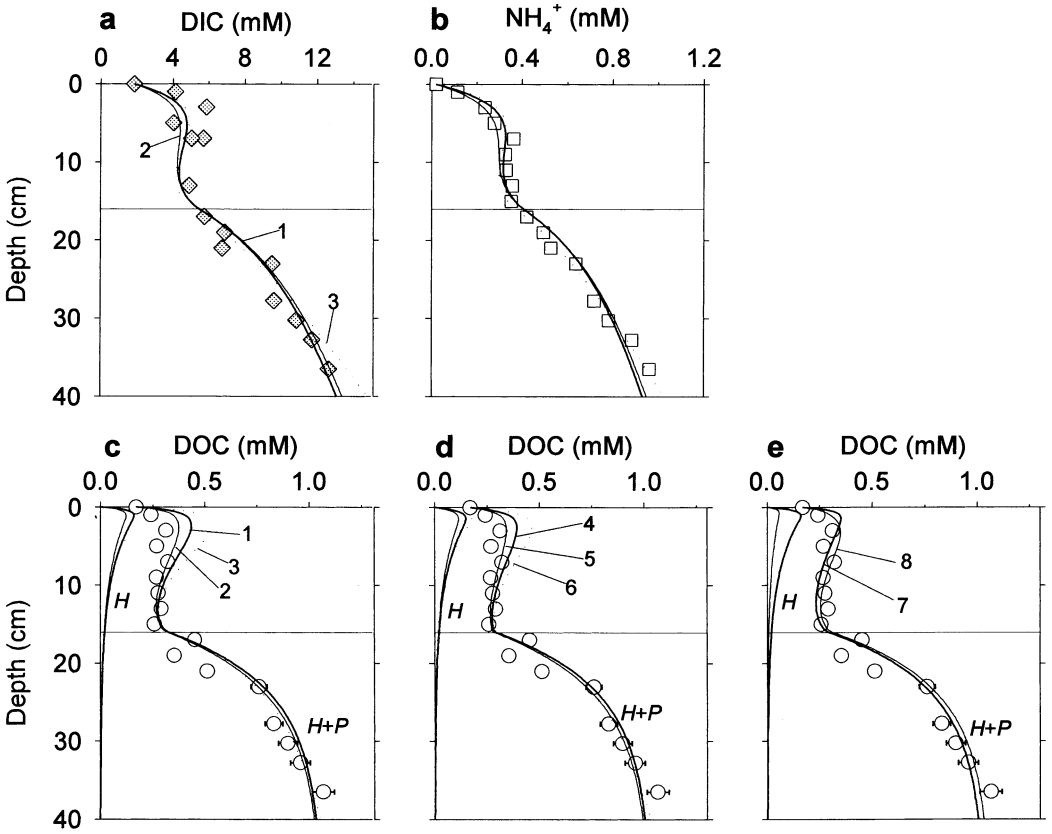

Fig. 6. Measured DIC, NH_4^+ and DOC profiles from Bay-3 (6/97) (replication of those given in Fig. 3) and model-derived profiles of *C*, *N*, *H* and *P* calculated with different parameter settings as given in Table 5 (numbers refer to Case numbers). Horizontal lines indicate the position of L. Error bars (where visible) represent ± 1 standard deviation.

coupled model to simultaneously solve for HMW-DOC, pLMW-DOC, DIC and NH_4^+. DIC and NH_4^+ were sensitive to variations in the unknown parameters (a, r_a, k_H, k_P, and r_{kp}), but the outputs did not differ significantly from those given in Figures 6a and 6b, unless under conditions that produced unreasonable DOC profiles. Therefore, from here on, only HMW- and pLMW-DOC profiles are reported.

As an initial condition, both r_a and r_{kp} were set to 1 (i.e., DOC reaction is independent of redox conditions). k_H was also initially set to 1000 yr^{-1}, which is similar in magnitude to degradation rate constants measured for dissolved free amino acids (Henrichs, 1992). Under these conditions, it was possible to assign multiple k_P-a combinations by balancing increased k_P (faster degradation of pLMW-DOC) with greater a (larger fraction of HMW-DOC supplies pLMW-DOC). The data could be adequately modeled by varying k_P between zero (i.e., pLMW-DOC is non-reactive) and the maximum value allowable without causing DOC to decrease with depth (beyond 40 cm). Because it is unlikely that pLMW-DOC is non-reactive, we report the maximum allowable k_P and its corresponding a. Values of k_P thus obtained should nevertheless be considered minimum estimates, because there is no a priori reason to believe that the reactivity of pore-water DOC does not decrease with depth in the sediment (Burdige, 2002).

The resulting DOC profiles for Case-1 to Case-3 are shown in Figure 6c. The model agreed well with the data at depths >10 cm when k_P was set to 3 to 4×10^{-3} yr^{-1}, and a to 0.03 to 0.05 (Table 5). The estimated range of k_P is ~1 order of magnitude $< k_{POC}$, but similar to POC degradation rate constants reported for pelagic sediments (Grundmanis and Murray, 1982; Jahnke et al., 1982; Table 5). The fact that a is on the order of 10^{-2} is consistent with the report that only ~3% of initial POC hydrolysis products escape fermentation to low molecular weight compounds in an anoxic coastal sediment (Alperin et al., 1994).

In contrast, within the uppermost 10 cm of the sediment column, the model consistently overestimated DOC. Only a part of this discrepancy can be explained if D_B is severely underestimated (Fig. 6d, Case-4 to Case-6). To determine whether redox-dependent production of P can explain the observed discrepancy, r_a in Case-1 was reduced to 0.3 above horizon L (Case-7). This reduced the concentration of pLMW-DOC above L allowing better fit with the data (Fig. 6e; statistical significance of this fit is given in Appendix B). In contrast, increasing r_{kp} even by 1000-fold exerted negligible impact on DOC near the sediment surface (data not shown). Alternatively, it was possible to simulate the data by increasing k_H to 3000 yr^{-1} (Fig. 6e, Case-8; see Appendix B for statistical analysis). Although enhanced H consumption (Case-8) cannot be refuted, the trend observed in the fluorescence data (Fig. 4) strongly suggests reduced production of pLMW-DOC above L (Case-7). Therefore, the model and data are consistent if production of pLMW-DOC is suppressed in the mixed-redox section of this sediment column.

4.2. Model Fit to a Non-Bioturbated/Non-Irrigated Site (Shelf-3)

Profiles obtained from station Shelf-3 were modeled as an example of a non-bioturbated/non-irrigated site. The H_2S profile from this station indicates that anoxic conditions prevailed below 3 cm depth (Fig. 3), hence L was initially set to 3 cm. As discussed above for Bay-3, DIC and NH_4^+ were first modeled independently of HMW- and pLMW-DOC to constrain R_0, R_{500}, and λ. Best-fit curves for DIC and NH_4^+ were obtained with R_0 ranging from 3.5×10^4 to 6.0×10^4 μmol/L yr^{-1} (Table 5, Figs. 7a and 7b; Case-9 to Case-11), with corresponding sediment POC reaction rate constants from 0.08 to 0.13 yr^{-1} (Table 5). Although these model outputs agreed reasonably well with measured values below 20 cm depth, the model profiles significantly overestimated DIC and NH_4^+ within the uppermost 15 to 20 cm (Figs. 7a and 7b) for unclear reasons. One potential explanation is that the effective molecular diffusion coefficient within the uppermost few cm of the sediment column was enhanced due to meiofaunal activity (Aller and Aller, 1992). Enhancement of molecular diffusivity within the uppermost 3 cm of the sediment by a factor of 2 (mid range reported for a coastal sediment by Aller and Aller, 1992) results in some improvement in the model fit to the DIC, NH_4^+ (with insignificant changes in R_0 and k_{POC}), and DOC profiles (data not shown). However, we default to the simpler case without meiofaunal activity, because the overall conclusions that we draw (see below) are largely unaffected by the presence or absence of such an enhancement factor.

To model HMW- and pLMW-DOC, the same initial conditions as those for Bay-3 ($r_a = r_{kp} = 1$; $k_H = 1000$ yr^{-1}) were first adopted. By setting a to ~0.02 and k_P to 10^{-4} to 10^{-3} yr^{-1}, DOC could be simulated reasonably well at depth, but deviated notably within the upper ~7 cm (Fig. 7c; Case-9 to Case-11). The model grossly underestimated DOC production at or near the sediment-water interface, and overestimated production (or underestimated consumption) to ~7 cm depth. Because this core was squeezed (Table 1), it is possible that the large interfacial DOC gradient was an artifact of whole-core squeezing (Martin and McCorkle, 1993). However, the general lack of benthic fauna in these sediments (section 2.1) suggests that such an effect was minimal (Alperin et al., 1999). We therefore interpret this to indicate locally-enhanced net production of HMW-DOC (rather than pLMW-DOC) at or near the sediment-water interface. Enhancement of HMW- over pLMW-DOC is supported by the fluorescence data (Fig. 7c), and also by previous findings pointing to enhanced production of labile dissolved organic matter near the sediment-water interface (Burdige and Zheng, 1998; Burdige, 2001).

Taking Case-9 as representative, k_H was reduced to 200 yr^{-1}as a means to capture the interfacial DOC gradient. This caused DOC to be overestimated to ~15 cm depth (Fig. 7d; Case-12). To determine whether this disagreement can be reduced through redox-dependent reaction of pLMW-DOC, r_{kp} was increased to 1000 above L (Case-13), but this effected only a minor change in the model DOC profile (Fig. 7e). Reducing r_a to 0.1 also exerted minimal impact on the DOC profile (data not shown).

Nevertheless, better agreement with the data, especially with the fluorescence profile, could be achieved when L was lowered from the inferred mixed-redox/anoxic boundary of 3 (Fig. 3) to 7 cm, while maintaining enhanced pLMW-DOC consumption ($r_{kp} = 1000$; Fig. 7f; Case-14). Almost identical results could also be obtained by simultaneously enhancing pLMW-DOC consumption and reducing pLMW-DOC production above L

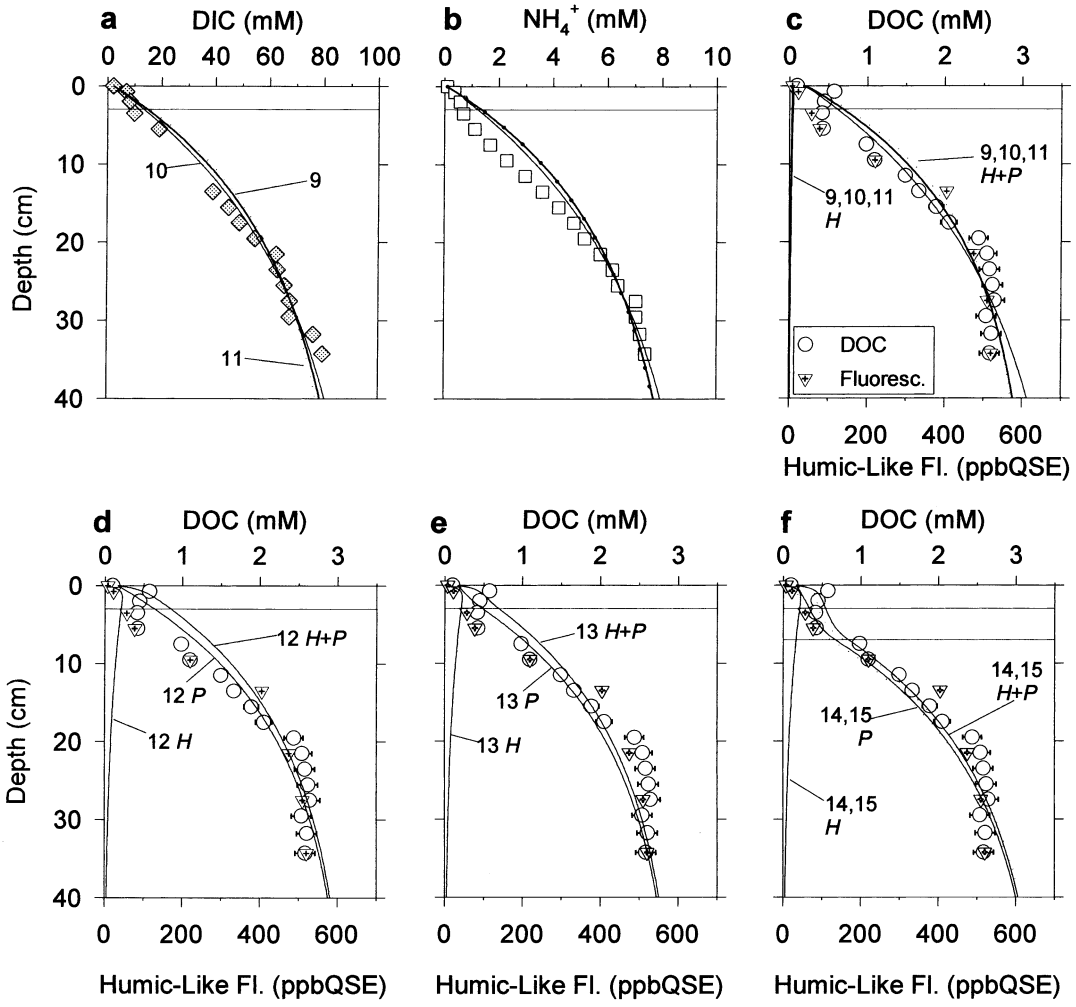

Fig. 7. Measured DIC, NH_4^+, DOC, and humic-like fluorescence profiles at Shelf-3 (replication of those given in Fig. 3) and model-derived profiles of *C*, *N*, *H* and *P* calculated with different parameter settings as given in Table 5 (numbers refer to Case numbers). Horizontal lines indicate the position of *L*. In panel f, solid and dotted indicate case 14 and 15, respectively. Error bars (where visible) represent ±1 standard deviation.

(r_a = 0.1, r_{kp} = 500; Fig. 7f, Case-15). This required deepening of *L* relative to the mixed-redox/anoxic boundary observed at the time of coring is justified if the boundary had shoaled within the recent past. Signs of surface sediment redistribution events at this site (section 2.1) suggest that the mixed-redox/anoxic boundary is subject to migration by several centimeters. Shoaling of the redox boundary may also be a sampling artifact, because temperature increases during core recovery and pressurization during squeezing (Table 1) may promote degassing of H_2S and CH_4 from deeper sections of the core. The oscillatory nature of the mixed-redox/anoxic boundary and the relatively low diffusivity of DOC (Table 4) may also explain why the depth interval within which DOC remained constant with depth penetrated beyond the observed redox boundary in several cores (Figs. 2 and 3, section 2.2.2).

If humic-like fluorescence intensity is indeed proportional to pLMW-DOC, then these results suggest that the coupled DOC-DIC-NH_4^+ model can predict with reasonable accuracy the depth distribution of the more refractory component of the DOC pool. These results are also consistent with the hypothesis that reduced production ($r_a < 1$) and enhanced loss ($r_{kp} > 1$) of the more refractory fraction of pore water DOC occurs in the mixed-redox parts of the sediment column. Furthermore, the fact that the current version of the model does not adequately reproduce the apparently large DOC gradient across the sediment-water interface points to the possibility that HMW-DOC can be produced at high rates, and possibly under non-steady state conditions, in the uppermost parts of the sediment column.

4.3. Redox-Dependent Sorption of DOC

So far, it was assumed that pore-water DOC distribution and cycling can be largely explained by incorporating the effects of redox-dependent microbial reactions, bioturbation/irrigation, sorption, and diffusion into a diagenetic model. While a combination of these factors appears reasonably adequate to explain the observed pore-water DOC distributions, additional factors

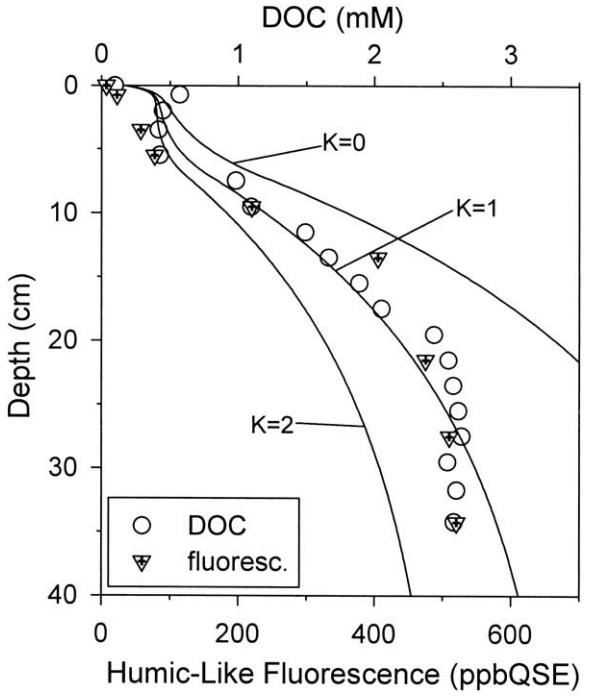

Fig. 8. Measured profiles of DOC and humic-like fluorescence, and model-derived profiles of the sum of H and P for station Shelf-3 (Case-15 to Case-17 in Table 5). $K = 1$ (Case-15) is a reproduction of the curve given in Figure 7f.

are most likely at work in nature. Here we discuss the potential role of redox-dependent sorption.

As seen in Eqn. 2, 3, and 5, including the equilibrium partition coefficient, K, in a steady state diagenetic equation under the conditions assumed in this study results in an enhancement of the rate of burial and bioturbation by a factor $(1 + K)$. Consequently, as stated by Berner (1976), when rates of burial and bioturbation are low enough to be neglected, effects of sorption can also be neglected. This appeared to be the case for station Bay-3 (6/97) where burial rates are low (0.15 cm yr^{-1}; Olsen et al., 1984), and high bioirrigation rates overwhelmed the impact of increasing D_B by a factor of 2 (data not shown). Hence, DOC distributions at Bay-3 (6/97) can be explained primarily as consequences of redox-dependent organic matter degradation and irrigation.

Conversely, at station Shelf-3 where sedimentation rates are on the order of several cm per year (Bopp et al., 1995) and bioirrigation is absent, the inclusion of K in the model has greater impact on the calculated DOC, with larger values of K resulting in lower DOC concentrations (Fig. 8). An accurate determination of K is therefore important to correctly model pore-water DOC under the conditions encountered at station Shelf-3. Furthermore, if K is indeed smaller in anoxic conditions as has been reported for some model compounds (Wang and Lee, 1993; Montluçon and Lee, 2001), then K must be modeled as a depth-dependent parameter. Redox-dependent sorption has also been suggested to significantly impact DOC accumulation in freshwater wetlands (Chin et al., 1998). Future studies should focus on determining the redox-dependence of K of pore-water DOC.

5. SUMMARY AND CONCLUSIONS

Pore-water DOC in Raritan–New York Bay complex and Inner New York Bight sediments increased steadily with depth in anoxic zones of the sediment column, but remained nearly constant (at concentrations higher than the bottom water values) under mixed-redox conditions. Fluorescence data indicated that humic-like compounds are a significant component of pore-water DOC throughout the depths examined, but particularly concentrated in the anoxic zone of the sediment.

Model predictions of DOC profiles for two stations consistently agreed with DOC data below an assigned mixed-redox/anoxic boundary, but gave notable deviations above. Below the mixed-redox/anoxic boundary, DOC could be modeled as being primarily comprised of poorly-reactive compounds (degradation rate constant on the order of 10^{-3} yr^{-1}). Three to four percent of the initial POC hydrolysis products appeared to escape mineralization to enter this refractory pool. The recalcitrant nature of DOC accumulating in pore waters is consistent with substrate-amended sediment incubation results that showed negligible net increase in pore-water DOC over a time course of 100 d (Hee et al., 2001).

In contrast, above the mixed-redox/anoxic horizon, DOC distributions were best described by assuming suppressed production and enhanced oxidation of refractory components. At the heavily bioirrigated station Bay-3, limited accumulation of refractory DOC may be explained as the result of a combined effect of oxidant availability and co-metabolism (Aller, 1994). At the non-bioturbated station Shelf-3, oxidant availability may be a more important factor. These findings appear consistent with the hypothesis that greater oxygen exposure results in lower organic matter preservation in marine sediments (Hartnett et al., 1998; Hedges et al., 1999).

Incorporation of the linear adsorption constant in model equations can impact calculated DOC profiles if sedimentation rates are high and bioirrigation rates are low. More research is needed to evaluate sorptive behavior of pore-water DOC under varying redox conditions.

Benthic DOC fluxes are an important component of the marine C cycle (Burdige et al., 1999; Holcombe et al., 2001). As such, the composition and reactivity of DOC leaving bottom sediments and entering the ocean's interior are of great interest. This study suggests that DOC effluxing from coastal sediments includes both labile and poorly-reactive moieties. Whether or not the less reactive component of the DOC leaving the benthos will persist in the oxic bottom waters over time scales relevant to the mixing time of the ocean (~1000 yr) remains to be tested (Burdige, 2002).

Acknowledgments—We thank M. Taillefert and T. Rozan for providing expert guidance for the solid phase Fe analyses, M. Buchholtz ten Brink for the bioturbation and sedimentation data, A. Draxler for the dissolved sulfide data, J. Gregg for the benthic invertebrate data, and H. Hartnett, W. Wang, and S. Boehme for help in the field and in the laboratory. We are grateful to J. Middelburg, F. Meysman, S. Beaupré, and three anonymous reviewers for insightful comments that significantly improve this manuscript. This work was funded by the National Undersea Research Program, Hudson River Foundation, and the Institute of Marine and Coastal Sciences at Rutgers.

Associate editor: J. J. Middelburg

REFERENCES

Aller R. C. (1994) Bioturbation and remineralization of sedimentary organic matter: effects of redox oscillation. *Chem. Geol.* 114, 331–345.

Aller R. C. and Aller J. Y. (1992) Meiofauna and solute transport in marine muds. *Limnol. Oceanogr.* 37, 1018–1033.

Alperin M. J., Albert D. B., and Martens C. S. (1994) Seasonal variations in production and consumption rates of dissolved organic carbon in an organic-rich coastal sediment. *Geochim. Cosmochim. Acta* 58, 4909–4930.

Alperin M. J., Martens C. S., Albert D. B., Suayah I. B., Benninger L. K., Blair N. E., and Jahnke R. A. (1999) Benthic fluxes and porewater concentration profiles of dissolved organic carbon in sediments from the North Carolina continental slope. *Geochim. Cosmochim. Acta* 63, 427–448.

Arnarson T. S. and Keil R. G. (2000) Mechanisms of pore water organic matter adsorption to montmorillonite. *Mar. Chem.* 71, 309–320.

Arnosti C. and Holmer M. (1999) Carbohydrate dynamics and contributions to the carbon budget of an organic-rich coastal sediment. *Geochim. Cosmochim. Acta* 63, 393–403.

Bauer J. E., Reimers C. E., Druffel E. R. M., and Williams P. M. (1995) Isotopic constraints on carbon exchange between deep ocean sediments and sea water. *Nature* 373, 686–689.

Berner R. A. (1976) Inclusion of adsorption in the modelling of early diagenesis. *Earth Planet. Sci. Lett.* 29, 333–340.

Berner R. A. (1980) *Early Diagenesis*. Princeton University Press, Princeton, NJ.

Bevington P. R. (1969) *Data Reduction and Error Analysis for the Physical Sciences*. McGraw-Hill, New York.

Bopp R. F., Robinson D. W., Simpson H. J., Biscaye P. E., Anderson R. F., Tong H., Monson S. J., and Gross M. L. (1995) Recent sediment and contaminant distributions in the Hudson Shelf Valley. In *Effects of the Cessation of Sewage Sludge Dumping at the 12-Mile Site (NOAA Tech. Rep. NMFS 124)* (eds. A. L. Strudholme, J. E. O'Reilly, and M. C. Ingham), pp. 61–82. U. S. Department of Commerce, Washington, DC.

Boudreau B. P. (1997) *Diagenetic Models and Their Implementation*. Springer-Verlag, New York.

Burdige D. J. (2001) Dissolved organic matter in Chesapeake Bay sediment pore waters. *Org. Geochem.* 32, 487–505.

Burdige D. J. (2002) Sediment pore waters. In *Biogeochemistry of Marine Dissolved Organic Matter* (eds. D. A. Hansell and C. A. Carlson), p. 774. Academic Press, San Diego, CA.

Burdige D. J. and Homstead J. (1994) Fluxes of dissolved organic carbon from Chesapeake Bay sediments. *Geochim. Cosmochim. Acta* 58, 3407–3424.

Burdige D. J. and Zheng S. (1998) The biogeochemical cycling of dissolved organic nitrogen in estuarine sediments. *Limnol. Oceanogr.* 43, 1796–1813.

Burdige D. J., Berelson W. M., Coale K. H., McManus J., and Johnson K. S. (1999) Fluxes of dissolved organic carbon from California continental margin sediments. *Geochim. Cosmochim. Acta* **63,** *10*, 1507–1515.

Burdige D. J., Kline S. W., and Chen W. (2004) Fluorescent dissolved organic matter in marine sediment pore waters. *Mar. Chem.* **89,** 289-311.

Chen R. F. and Bada J. L. (1989) Seawater and porewater fluorescence in the Santa Barbara Basin. *Geophys. Res. Lett.* 16, 687–690.

Chen R. F. and Bada J. L. (1994) The fluorescence of dissolved organic matter in porewaters of marine sediments. *Mar. Chem.* 45, 31–42.

Chen R. F., Bada J. L., and Suzuki Y. (1993) The relationship between dissolved organic carbon (DOC) and fluorescence in anoxic marine pore waters: Implications for estimating benthic DOC fluxes. *Geochim. Cosmochim. Acta* 57, 2149–2153.

Chin Y.-P. and Gschwend P. M. (1991) The abundance, distribution, and configuration of porewater organic colloids in recent sediments. *Geochim. Cosmochim. Acta* 55, 1309–1317.

Chin Y.-P., Traina S. J., and Swank C. R. (1998) Abundance and properties of dissolved organic matter in pore waters of a freshwater wetland. *Limnol. Oceanogr.* 43, 1287–1296.

Cline J. D. (1969) Spectrophotometric determination of hydrogen sulfide in natural waters. *Limnol. Oceanogr.* 14, 454–458.

Coble P. G. (1996) Characterization of marine and terrestrial DOM in seawater using excitation-emission matrix spectroscopy. *Mar. Chem.* 51, 325–346.

Craig, H. (1974) A scavenging model for trace elements in the deep sea. *Earth Planet. Sci. Lett.* **23,** 149–159.

Cutter G. A. and Oatts T. J. (1987) Determination of dissolved sulfide and sedimentary sulfur speciation using gas chromatography-photoionization detection. *Anal. Chem.* 59, 717–721.

Emerson S., Jahnke R., and Heggie D. (1984) Sediment-water exchange in shallow water estuarine sediments. *J. Mar. Res.* 42, 709–730.

Grundmanis V. and Murray J. W. (1982) Aerobic respiration in pelagic marine sediments. *Geochim. Cosmochim. Acta* 46, 1101–1120.

Hall P. O. J. and Aller R. C. (1992) Rapid, small-volume, flow injection analysis for ΣCO_2 and NH_4^+ in marine and freshwaters. *Limnol. Oceanogr.* 37, 1113–1119.

Harris C. K., Butman B., and Traykovski P. (2003) Winter-time circulation and sediment transport in the Hudson Shelf Valley. *Cont. Shelf. Res.* 23, 801–820.

Hartnett H. E., Keil R. G., Hedges J. I., and Devol A. H. (1998) Influence of oxygen exposure time on organic carbon preservation in continental margin sediments. *Nature* 391, 572–537.

Hedges J. I., Hu F. S., Devol A. H., Hartnett H. E., Tsamakis E., and Keil R. G. (1999) Sedimentary organic matter preservation: a test for selective degradation under oxic conditions. *Am. J. Sci.* 299, 529–555.

Hedges J. I. and Keil R. G. (1995) Sedimentary organic matter preservation: An assessment and speculative synthesis. *Mar. Chem.* 49, 81–115.

Hee C. A., Pease T. K., Alperin M. J., and Martens C. S. (2001) Dissolved organic carbon production and consumption in anoxic marine sediments: A pulsed-tracer experiment. *Limnol. Oceanogr.* 46, 1908–1920.

Henrichs S. M. (1992) Early diagenesis of organic matter in marine sediments: Progress and perplexity. *Mar. Chem.* 39, 119–149.

Henrichs S. M. and Farrington J. W. (1979) Amino acids in interstitial waters of marine sediments. *Nature* 279, 319–322.

Holcombe B. L., Keil R. G., and Devol A. H. (2001) Determination of pore-water dissolved organic carbon fluxes from Mexican margin sediments. *Limnol. Oceanogr.* 46, 298–308.

Jahnke R. A. (1988) A simple, reliable, and inexpensive pore-water sampler. *Limnol. Oceanogr.* 33, 483–487.

Jahnke R., Heggie D., Emerson S., and Grundmanis V. (1982) Pore waters of the central Pacific Ocean: nurient results. *Earth Planet. Sci. Lett.* 61, 233–256.

Komada T. and Reimers C. E. (2001) Resuspension-induced partitioning of organic carbon between solid and solution phases from a river-ocean transition. *Mar. Chem.* 76, 155–174.

Komada T., Schofield O. M. E., and Reimers C. E. (2002) Fluorescence characteristics of organic matter released from coastal sediments during resuspension. *Mar. Chem.* 79, 81–97.

Kostka J. E. and Luther G. W., III. (1994) Partitioning and speciation of solid phase iron in saltmarsh sediments. *Geochim. Cosmochim. Acta* **58,** 1701–1710.

Laane R. W. P. M. and Koole L. (1982) The relationship between fluorescence and dissolved organic carbon in the Ems-Dollart estuary and the western Wadden Sea. *Neth. J. Sea Res.* 15, 217–227.

Li Y.-H. and Gregory S. (1974) Diffusion of ions in sea water and in deep-sea sediments. *Geochim. Cosmochim. Acta* 38, 703–714.

Luther G. W., III, Ferdelman T. G., Kostka J. E., Tsamakis E. J., and Church T. M. (1991) Temporal and spatial variability of reduced sulfur species (FeS_2, $S_2O_3^{2-}$) and porewater parameters in salt marsh sediments. *Biogeochemistry* **14,** 57–88.

Luther G. W., III, Reimers C. E., Nuzzio D. B., and Lovalvo D. (1999) In situ deployment of voltammetric, potentiometric, and amperometric microelectrodes from a ROV to determine dissolved O_2, Mn, Fe, S(−2), and pH in porewaters. *Environ. Sci. Technol.* **33,** 4352–4356.

Mackin J. A. and Aller R. C. (1984) Ammonium adsorption in marine sediments. *Limnol. Oceanogr.* **29,** *2*, 250–257.

Martin W. R. and McCorkle D. C. (1993) Dissolved organic carbon concentrations in marine pore waters determined by high-temperature oxidation. *Limnol. Oceanogr.* 38, 1464–1479.

Middelburg J. J., Soetaert K., and Herman P. M. J. (1997) Empirical relationships for use in global diagenetic models. *Deep-Sea Res.* 44, 327–344.

Montluçon D. B. and Lee C. (2001) Factors affecting lysine sorption in a coastal sediment. *Org. Geochem.* 32, 933–942.

Olsen C. R., Larsen I. L., Brewster R. H., Cutshall N. H., Bopp R. F., and Simpson H. J. (1984) *A Geochemical Assessment of Sedimentation and Contaminant Distributions in the Hudson-Raritan Estuary*. National Oceanic and Atmospheric Administration, Washington, DC.

Sansone F. J. and Martens C. S. (1982) Volatile fatty acid cycling in organic-rich marine sediments. *Geochim. Cosmochim. Acta* 46, 1575–1589.

Sharp J. H., Benner R., Bennett L., Carlson C. A., Dow R., and Fitzwater S. E. (1993) Re-evaluation of high temperature combustion and chemical oxidation measurements of dissolved organic carbon in seawater. *Limnol. Oceanogr.* 38, 1774–1782.

Sholkovitz E. R. and Mann D. R. (1984) The pore water chemistry of ^{239,240}Pu and ^{137}Cs in sediments of Buzzards Bay, Massachusetts. *Geochim. Cosmochim. Acta* 48, 1107–1114.

Stookey L. L. (1970) Ferrozine—A new spectrophotometric reagent for iron. *Anal. Chem.* 42, 779–781.

Thimsen C. A. and Keil R. G. (1998) Potential interactions between sedimentary dissolved organic matter and mineral surfaces. *Mar. Chem.* 62, 65–76.

Wang X.-C. and Lee C. (1993) Adsorption and desorption of aliphatic amines, amino acids and acetate by clay minerals and marine sediments. *Mar. Chem.* 44, 1–23.

APPENDIX A

Analyte	Method	Precision[a]	References and Comments[b]
DIC	Flow-injection and conductivity analysis	3%	Hall and Aller (1992)
DOC	High-temperature catalytic oxidation	5%	Determined using a Shimadzu 5000A TOC Analyzer following recommendations by Sharp et al. (1993) (Komada and Reimers, 2001)
NH_4, PO_4	Spectrophotometry	3%	Determined using an automated analyzer (Quick Chem AE, Lachat Instruments)
Tot. Fe	Spectrophotometry	2%	Stookey (1970) with modifications described by Luther et al. (1991)
Tot. Mn	Graphite furnace atomic absorption spectrometry	3%	Determined using the method of standard additions
Humic-like fluorescence	Excitation-emission matrix spectroscopy	2%	Intensity of maximum emission at maximum excitation reported in equivalents of 1 ppb quinine bisulfate in 0.05 mol/L H_2SO_4 (Komada et al., 2002)
Tot. H_2S	Spectrophotometry	n.a.	Cline (1969)
Fe oxy-hydroxides	Ascorbate and dithionite extractions followed by determination of total dissolved Fe	<10%	Determined in duplicate according to Kostka and Luther (1994); dissolved Fe was determined according to Stookey (1970)
Acid volatile sulfide (AVS)	Acidification followed by trapping and quantitation of H_2S	<20%	Determined in triplicate according to Cutter and Oatts (1987) with modifications to the trapping and quantification procedures of H_2S as described by Luther et al. (1991)

[a] Relative standard deviation.

[b] DOC and fluorescence samples were collected in pre-cleaned (soap and acid), pre- combusted glass vials with Teflon-lined caps. Dissolved metal and nutrient samples were collected in pre-cleaned (soap and acid) HDPE vials.

APPENDIX B

Modeling the data by assuming $r_a \neq 1$ or $k_H \neq 1000$ adds another adjustable fitting parameter to the model. While such an approach will always improve the fit of the model to the data, the improvement may not be statistically significant (i.e., may occur simply by chance). The statistical significance of the improved fit of Case-7 and Case-8 relative to Case-1 can be evaluated using the F_χ ratio test (Bevington, 1969; Craig, 1974):

$$F_\chi = (n - p)\left[\frac{SS_{(\text{Case}-1)}}{SS_{(\text{Case}-7\text{ or }8)}} - 1\right] \quad (7)$$

where n is the number of pore-water DOC data points (18), p is the total number of free parameters that are constrained using the DOC data after adding the additional fitting parameter, and SS is the sum of squares of the residuals between the model and the data for the cases with (Case-7 or Case-8) and without (Case-1) redox-dependent DOC reaction. For both Case-7 and Case-8, p is equal to 3 (k_P, a, r_a in Case-7, and k_H, k_P, a in Case-8; Table 5). The SS for Case-1, Case-7, and Case-8 are 0.159, 0.0951, and 0.102, respectively, giving an F_χ statistic of 10.0 for Case-7 and 8.4 for Case-8. For $N - p$ degrees of freedom, F_χ is inversely related to the probability P_F that the observed improvement in the fit of the model to the data occurred by chance (Bevington, 1969). For Case-7 and Case-8, P_F is <1 and <2.5% respectively, indicating that the improved fit to the model to the data by the addition of a redox-dependent reaction parameter was significant.